A Distinct Pathway for Polar Exocytosis in Plant Cell Wall Formation[1][OPEN]

Hao Wang[2], Xiaohong Zhuang[2], Xiangfeng Wang, Angus Ho Yin Law, Teng Zhao, Shengwang Du, Michael M.T. Loy, and Liwen Jiang*

School of Life Sciences, Centre for Cell and Developmental Biology and State Key Laboratory of Agrobiotechnology, The Chinese University of Hong Kong, Shatin, New Territories, Hong Kong, China (H.W., X.Z., X.W., A.H.Y.L., L.J.); College of Life Sciences, South China Agricultural University, Guangzhou 510642, China (H.W.); Department of Physics, The Hong Kong University of Science and Technology, Clear Water Bay, Kowloon, Hong Kong, China (T.Z., S.D., M.M.T.L.); Division of Biomedical Engineering, The Hong Kong University of Science and Technology, Clear Water Bay, Kowloon, Hong Kong, China (S.D.); and CUHK Shenzhen Research Institute, The Chinese University of Hong Kong, Shenzhen 518057, China (L.J.)

Post-Golgi protein sorting and trafficking to the plasma membrane (PM) is generally believed to occur via the trans-Golgi network (TGN). In this study using *Nicotiana tabacum* pectin methylesterase (NtPPME1) as a marker, we have identified a TGN-independent polar exocytosis pathway that mediates cell wall formation during cell expansion and cytokinesis. Confocal immunofluorescence and immunogold electron microscopy studies demonstrated that Golgi-derived secretory vesicles (GDSVs) labeled by NtPPME1-GFP are distinct from those organelles belonging to the conventional post-Golgi exocytosis pathway. In addition, pharmaceutical treatments, superresolution imaging, and dynamic studies suggest that NtPPME1 follows a polar exocytic process from Golgi-GDSV-PM/cell plate (CP), which is distinct from the conventional Golgi-TGN-PM/CP secretion pathway. Further studies show that ROP1 regulates this specific polar exocytic pathway. Taken together, we have demonstrated an alternative TGN-independent Golgi-to-PM polar exocytic route, which mediates secretion of NtPPME1 for cell wall formation during cell expansion and cytokinesis and is ROP1-dependent.

Plant development and growth require coordinated tissue and cell polarization. Two of the most essential cellular processes involved in polarization are cell expansion and cytokinesis, which determines cell morphology and functions (Jaillais and Gaude, 2008; Dettmer and Friml, 2011; Li et al., 2012). Pollen tube and root hair growth require highly polarized membrane trafficking (Libault et al., 2010; Kroeger and Geitmann, 2012). Cytokinesis, by which new cells are formed, separates daughter cells by forming a new structure within the cytoplasm termed the cell plate (CP). Made up of a cell wall (CW), surrounded by new plasma membrane (PM), the cell plate is generally considered to be an example of internal cell polarity in a non-polarized plant cell (Bednarek and Falbel, 2002; Baluska et al., 2006).

The conventional view of pollen tube tip growth and cell plate formation is supported by polar exocytic secretion of numerous vesicles (diameter of 60–100 nm) to the pollen tube tip and phragmoplast areas during cytokinesis. These polar exocytic vesicles, which are generally believed to originate from the Golgi apparatus, are delivered to the site of secretion via the cytoskeleton and fuse with the target membrane with the aid of fusion factors (Jurgens, 2005; Backues et al., 2007). However, whether these polar exocytic vesicles undergoing post-Golgi trafficking are part of the conventional Golgi-trans-Golgi network (TGN)-PM/CP exocytosis or are derived from some other unidentified exocytic secretion pathway remain unclear.

Polar exocytosis is regulated and controlled by a conserved Rho GTPase signaling network in fungi, animals, and plants (Burkel et al., 2012; Ridley, 2013). Rho of plant (ROP), the sole subfamily of Rho GTPases in plant, participate in signaling pathways that regulate cytoskeleton organization and endomembrane

[1] This work was supported by grants from the Research Grants Council of Hong Kong (CUHK466011, 465112, 466613, CUHK2/CRF/11G, C4011-14R, HKUST10/CRF/12R, and AoE/M-05/12), NSFC/RGC (N_CUHK406/12), NSFC (31470294), Croucher-CAS Joint Lab, and Shenzhen Peacock Project (KQTD201101) to L.J. This work was also supported by NSFC (31570001) and Natural Science Foundation of Guangdong Province (2016A030313401) to H.W., HKUST VPRGO12SC02 grant to M.M.T.L., and by the grant HKUST12/CRF/13G from the Research Grants Council of Hong Kong to M.M.T.L., S.D., and L.J.

[2] These authors contributed equally to the article.

* Address correspondence to ljiang@cuhk.edu.hk.

The author responsible for distribution of materials integral to the findings presented in this article in accordance with the policy described in the Instructions for Authors (www.plantphysiol.org) is: Liwen Jiang (ljiang@cuhk.edu.hk).

H.W. and L.J. conceived the study; H.W. and X.Z. conducted most of the research; H.W., X.Z., X.W., and A.H.Y.L. analyzed the data; H.W., T.Z., S.D., and M.M.T.L. performed STORM imaging and image reconstruction; H.W. and L.J. wrote the manuscript; L.J. supervised the project.

[OPEN] Articles can be viewed without a subscription.

www.plantphysiol.org/cgi/doi/10.1104/pp.16.00754

trafficking, consequently determining cell polarization, polar growth and cell morphogenesis (Gu et al., 2005; Lee et al., 2008). In growing pollen tubes, ROP1 participates in regulating polar exocytosis in the tip region via two downstream pathways to regulate apical F-actin dynamics: RIC4-mediated F-actin polymerization and RIC3-mediated apical actin depolymerization. A constitutively active mutant of ROP1 (CA-rop1) prevents fusion of these vesicles with the PM and enhances the accumulation of exocytic vesicles in the apical cortex of pollen tubes (Lee et al., 2008). Although ROP GTPases have been extensively researched, their roles in polar membrane expansion in pollen tubes and epidermal pavement cells remains unclear (Xu et al., 2010; Yang and Lavagi, 2012), and there have been insufficient studies on the functions of ROPs in controlling cell plate formation during cytokinesis. Cell division requires precise regulation and spatial organization of the cytoskeleton for delivery of secretion vesicles to the expanding cell plate (Molendijk et al., 2001).

In addition, newly made cell walls during cell expansion and cell plate formation require sufficient plasticity in order to integrate new membrane materials to support the polarized membrane extension. They also should be strong enough to withstand the internal turgor pressure and thereby maintain the shape of the cell (Zonia and Munnik, 2011; Hepler et al., 2013). Recent studies have demonstrated that pectins are important for both cytokinesis and cell expansion (Moore and Staehelin, 1988; Bosch et al., 2005; Chebli et al., 2012; Altartouri and Geitmann, 2015; Bidhendi and Geitmann, 2016). Pectins are one of the major cell wall components of the middle lamella and primary cell wall. They are polymerized and methylesterified in the Golgi and subsequently released into the apoplastic space as "soft" methylesterified polymers. The homogalacturonan components of pectin are later demethylesterified by pectin methylesterases (PMEs). The demethylesterified pectins can be cross-linked, interact with Ca^{2+}, and finally form the "hard" pectin matrix of the cell wall. Therefore, the enzymatic activity of PMEs determines the rigidity of the cell wall (Micheli, 2001; Peaucelle et al., 2011).

In Arabidopsis (*Arabidopsis thaliana*) and tobacco (*Nicotiana tabacum*) pollen tubes, PMEs are found predominantly polar localized in the tip region and determine the rigidity of the apical cell wall (Bosch et al., 2005; Jiang et al., 2005; Fayant et al., 2010; Chebli et al., 2012; Wang et al., 2013). PME isoform knockout mutants in Arabidopsis (*AtPPME1* or *vanguard1*) produce unstable pollen tubes which burst when germinated in vitro and have reduced fertilization abilities (Jiang et al., 2005; Rockel et al., 2008). Recent studies have shown that in growing tobacco pollen tubes, polar targeting of NtPPME1 to the pollen tube apex depends on an apical F-actin mesh network (Wang et al., 2013). Although the functions of PME in cell wall constriction are well documented, the intracellular secretion and regulation mechanism of the exocytic process of PME still remain largely unexplored. In addition, pectins are also found to be abundant in the forming cell plate, raising the possibility that PMEs may also function during cell plate formation (Moore and Staehelin, 1988; Dhonukshe et al., 2006).

In our study, we have used NtPPME1 as a marker to identify a polar exocytic process which is distinct from the conventional Golgi-TGN-PM exocytosis pathway in both pollen tube tip growth and cell plate formation. We have identified a Golgi-derived secretory vesicle (GDSV) for the polar secretion and targeting of NtPPME1 to the cell wall that bypasses the TGN during cell polarization. Further investigations using ROP1 mutants have shown that this polar exocytosis is ROP1 dependent.

RESULTS

Polar Exocytic Secretion of NtPPME1 to the Pollen Tube Tip

Nicotiana tabacum pollen-specific pectin methylesterase (NtPPME1), which is regulated by apical F-actin, plays a key role in pollen tube cell wall formation (Bosch et al., 2005; Bosch and Hepler, 2006; Wang et al., 2013). However, the details of post-Golgi intracellular secretion of NtPPME1 remain unclear. To explore the subcellular localization and to identify the endomembrane compartments mediating polar secretion of NtPPME1, we first raised an antibody specific against NtPPME1. The specificity the NtPPME1 antibodies was initially tested via protein gel blot analysis. As shown in Figure 1A, affinity-purified NtPPME1 antibodies detected a major band at ~60 kD, the expected size of NtPPME1, in total protein extracts from 2-h in vitro germinated tobacco pollen tubes. As the background control, preserum of NtPPME1 antibody was tested and showed no detection in western, immunofluorescent labeling and immunoEM (Supplemental Fig. S1). To further confirm the specificity of NtPPME1 antibody, pollen tubes expressing NtPPME1-GFP were used for protein extraction and western blot analysis using NtPPME1 and GFP antibodies. Both fusion protein and endogenous proteins can be specifically recognized (Supplemental Fig. S1A). Ideally, the specificity of the antibodies used in this study should be further confirmed via using proper mutants in future studies.

The tip-focused subcellular localization of NtPPME1 was shown via transient expression of NtPPME1-GFP fusion protein in growing pollen tubes and confocal immunofluorescence in fixed tobacco pollen tubes. As shown in Figure 1B, the growing pollen tube expressing NtPPME1-GFP via particle bombardment showed punctate dots in the cytosol and on the surface of the pollen tube tip. The NtPPME1 antibodies also labeled the pollen tube apical region and punctate dots in the cytosol (Fig. 1C). Such a distribution pattern is consistent with results obtained by transient expression of the

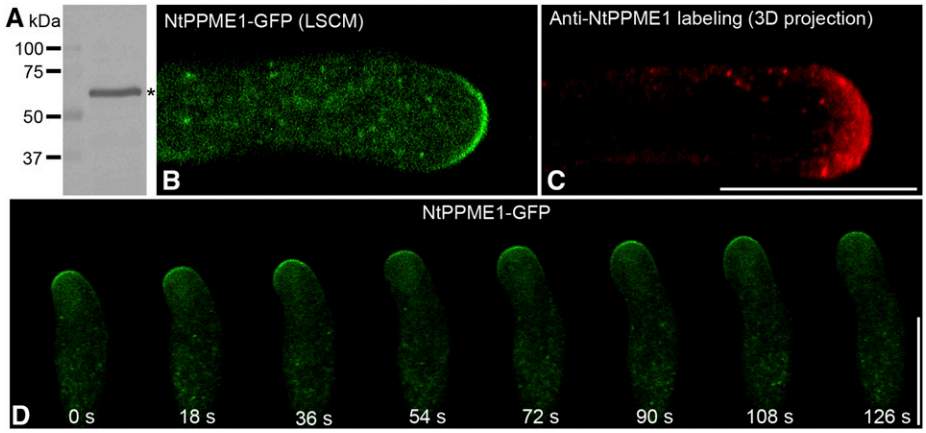

Figure 1. Polar exocytosis of NtPPME1 in the pollen tube tip. A, Characterization of NtPPME1 antibodies with total protein from 2-h germinated tobacco pollen tubes. The asterisk indicates the expected size of NtPPME1. M, Molecular mass in kilodaltons. B, Laser scanning of confocal microscopy (LSCM) image of a growing tobacco pollen tube expressing NtPPME1-GFP. C, Immunofluorescence labeling of NtPPME1 in tobacco pollen tube by using NtPPME1 antibodies. Scale bar = 25 μm. D, A representative time-lapse image series of expressing NtPPME1-GFP during pollen tube tip expansion. The fluorescent signals of NtPPME1-GFP remained tip-focused along with some intracellular punctate dots in the growing pollen tube. Scale bar = 25 μm.

NtPPME1-GFP fusion protein in pollen tubes. A representative time-lapse image series of expressing NtPPME1-GFP in the growing pollen tube was shown in Figure 1D. The fluorescent signals of NtPPME1-GFP constantly remained on the pollen tube apex during the tip expansion. In addition to the fluorescent signals detected in the pollen tube tip, punctate signals were also found within the cytoplasm of the pollen tubes expressing NtPPME1-GFP. The cytoplasmic organelles labeled by the NtPPME1-GFP were highly dynamic and mobile, moving along with the cytoplasmic streaming from distal to the tip region (Supplemental Movie S1).

NtPPME1-GFP-Positive Compartments Are Distinct from Conventional Post-Golgi Trafficking Endosomal Compartments

To better characterize the nature of the NtPPME1-GFP-positive organelle in growing pollen tubes, we compared its localization with other post-Golgi trafficking organelle markers. As shown in Supplemental Figure S2, A to E, the major signals of NtPPME1-GFP in growing tobacco pollen tubes were observed to be closely associated with, but not colocalized with, the trans-Golgi marker (RFP-GONST1). They were also separated from the PVC marker (RFP-AtVSR2), the cis-Golgi marker (RFP-ManI), the TGN marker (RFP-AtSCAMP4), and endocytic vesicles (FM4-64 dye after 10-min uptake).

Next, we used pharmaceutical treatments to further elucidate the identity of the NtPPME1-containing compartments including the following: (1) Brefeldin A (BFA), an ARF-GEF inhibitor, has been shown to induce Golgi and TGN aggregations in various plant cell types including pollen tubes and BY2 cells (Emans et al., 2002; Robinson et al., 2008; Lam et al., 2009; Wang et al., 2010a; Wang et al., 2011b); (2) wortmannin, a phosphoinositide 3-kinase inhibitor that causes homotypic fusion of PVCs (Ethier and Madison, 2002; Tse et al., 2004; Wang et al., 2009; Scheuring et al., 2011; Wang et al., 2011b; Gao et al., 2014a; Zhao et al., 2015; Cui et al., 2016); and (3) concanamycin A (ConcA), which is a V-ATPase inhibitor and prevents post-TGN trafficking resulting in early endosome aggregations (Robinson et al., 2004; Cai et al., 2011; Scheuring et al., 2011). These drugs are extensively used and regarded as useful tools in studying and dissecting endomembrane sorting and trafficking in eukaryotic cells. Although the apical localization of NtPPME1-GFP was interrupted after the pharmaceutical treatments, which might be due to pollen tube growth arrest and loss of cell polarity, our results showed that NtPPME1-GFP-positive intracellular compartments were insensitive to BFA, wortmannin, and ConcA treatments (Fig. 2, A–D) when compared with the responses of the TGN (GFP-AtSCAMP4) and PVC (GFP-AtVSR2) markers (Fig. 2, E–J). GFP-AtSCAMP4 showed typical aggregations after 15-min BFA and ConcA treatments, respectively, but remained punctate after 15-min wortmannin treatment (Fig. 2, E–H). Quantifications of the effects of drug treatment in pollen tubes are given in Supplemental Figure S3. These results are consistent with previous observations on the responses of the TGN to BFA and ConcA treatments (Lam et al., 2007a; Viotti et al., 2010; Wang et al., 2010a; Cai et al., 2011). After 15-min wortmannin treatment, GFP-AtVSR2 showed the typical enlarged ring-like structures (Fig. 2, I and J). These results indicate that NtPPME1 are delivered in a polar fashion to the pollen tube tip via a different post-Golgi organelle, which is distinct from the TGN and PVC.

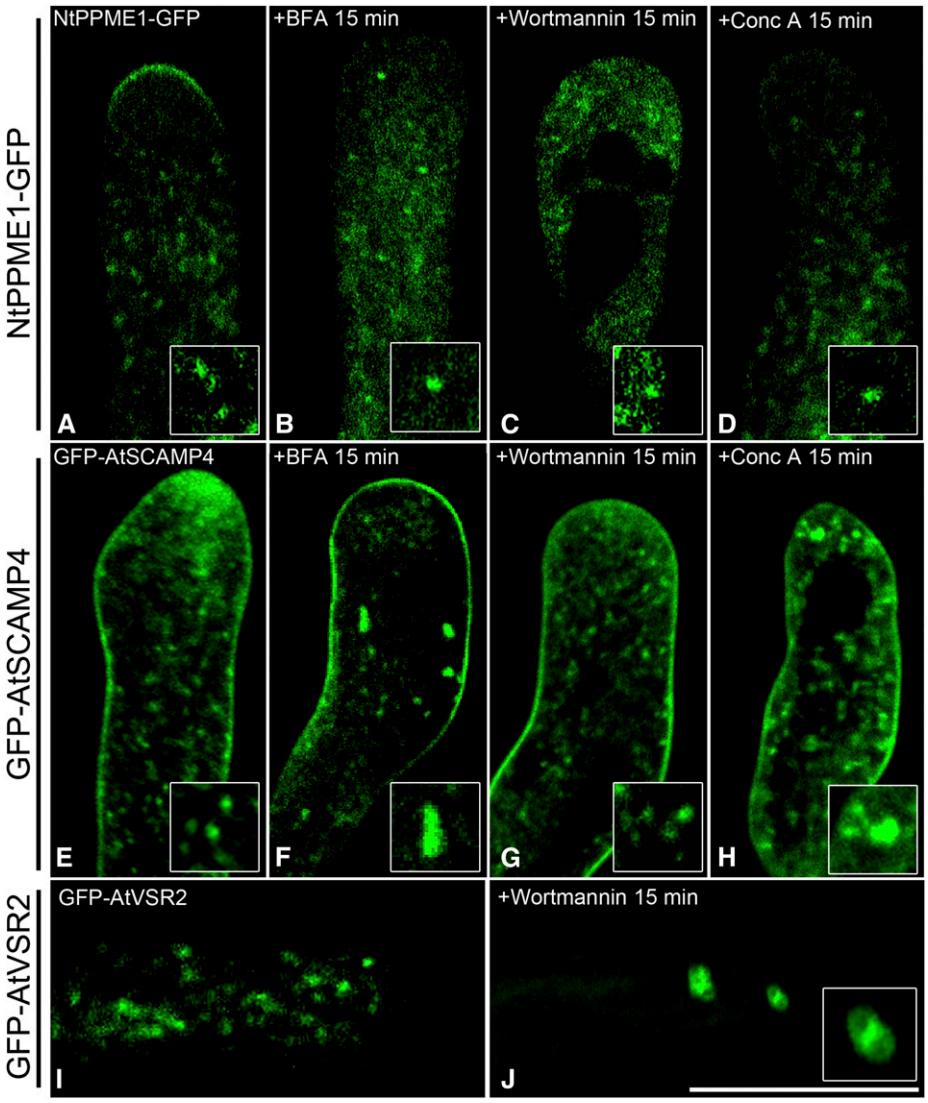

Figure 2. NtPPME1-GFP-positve compartments are insensitive to pharmaceutical treatments in pollen tubes. A to D, Growing pollen tubes expressing NtPPME1-GFP were treated with 10 μg mL^{-1} BFA (B), 8.25 μM wortmannin (C), and 2 μM ConcA (D) for 15 min respectively. E to H, Pollen tubes expressing GFP-AtSCAMP4 (TGN marker) formed aggregates after BFA and ConcA treatment for 15 min. I and J, Pollen tubes expressing GFP-AtVSR2 (PVC marker) were treated with wortmannin for 15 min and formed enlarged ring-like structures (J). Scale bar = 25 μm.

NtPPME1 Highlights the Forming Cell Plate during Cytokinesis and Is Distinct from Conventional Post-Golgi Trafficking Organelles in Tobacco BY2 Cells

Pectins are important to cell expansion during pollen tube growth. In addition, recent studies have demonstrated that pectins are essential to cytokinesis, with pectin demethylesterification being catalyzed by the PMEs (Moore and Staehelin, 1988; Micheli, 2001; Bosch et al., 2005; Dhonukshe et al., 2006; Peaucelle et al., 2011). The forming cell plate is regarded as an example of "inner cell polarity" in nonpolarized plant cells (Jurgens, 2005; Backues et al., 2007; Mravec et al., 2011). Although pectins are abundant in the forming cell plate, how PMEs function at the cell plate remains unclear (Micheli, 2001; Backues et al., 2007; Peaucelle et al., 2011). *NtPPME1* was highly expressed during cell plate formation in growing pollen tubes (Supplemental Fig. S4). Stable transgenic tobacco BY2 cells expressing NtPPME1-GFP were generated as a prerequisite for testing whether NtPPME1 is involved cell plate formation during cytokinesis. As shown in Figure 3A, the NtPPME1-GFP signals accumulated in the forming cell plate with some punctate dots in the cytosol (Supplemental Movie S2). While in the nondividing BY2 cells without polarity, the NtPPME1-GFP proteins were delivered into the vacuole for degradation (Fig. 3B). However, when compared with BY2 cells expressing a TGN marker (GFP-AtSCAMP4), which also highlights the forming cell plate, the dynamic responses of NtPPME1-GFP to different pharmaceutical treatments were distinct from that of GFP-AtSCAMP4 in BY2 cells. In Figure 3, C to F, within 30 min of treatments with BFA, ConcA, and wortmannin, respectively, the pattern of NtPPME1-GFP showed no significant changes, while GFP-AtSCAMP4 formed large aggregations after BFA and ConcA treatments representing the typical responses of early endosome to the treatment as previously reported (Lam et al., 2007a; Viotti et al., 2010; Cai et al., 2011). Quantifications of the

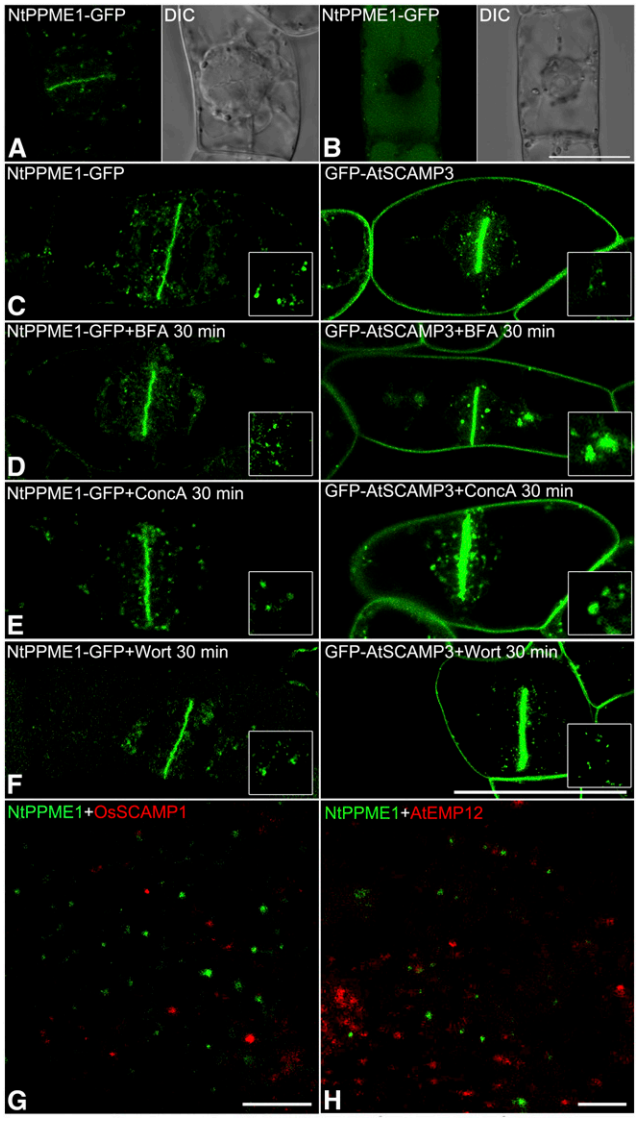

Figure 3. Polarity-associated NtPPME1 highlights cell plate during cytokinesis and is insensitive to BFA, ConcA, and wortmannin in tobacco BY2 cells. A and B, NtPPME1-GFP is polarity-associated and highlights the forming cell plate during cytokinesis in transgenic tobacco BY2 cells but degraded in the vacuole of a nondividing cell without polarity (B). C, Transgenic tobacco BY2 cells expressing both NtPPME1-GFP and GFP-AtSCAMP3 highlight cell plate during cytokinesis. D to F, Distinct responses of transgenic tobacco BY2 cells expressing NtPPME1-GFP and GFP-AtSCAMP3 to 10 μg mL^{-1} BFA, 2 μM ConcA, or 8.25 μM wortmannin 30-min treatment. Scale bar = 50 μm. G and H, Super resolution imaging by using STORM. BY2 cells were fixed and double-immunolabeled with NtPPME1 and OsSCAMP1 or AtEMP12 antibodies, respectively. Scale bar = 400 nm.

effects of drug treatment in BY2 cells are shown in Supplemental Figure S3. Because of the 200 nm resolution limit of the conventional laser scanning confocal microscopy, we performed superresolution imaging using stochastic optical reconstruction microscopy (STORM) to further confirm that NtPPME1-GFP-positive organelles are distinct from the TGN and Golgi apparatus. BY2 cells were fixed and double-immunolabeled with NtPPME1 and OsSCAMP1 or AtEMP12 antibodies. After image acquisition and reconstruction, NtPPME1-labeled cytosolic organelles were separate from TGNs and the Golgi apparatus (Fig. 3, G and H).

In addition to the secretory activity at the cell plate via the biosynthetic pathway, endocytic trafficking is also directed and contributes to cell plate formation (Dhonukshe et al., 2006; Boutte et al., 2010). The endocytic tracer FM4-64 is incorporated into developing cell plates, suggesting that endocytosed material is delivered to the initiating and expanding cell plates (Dhonukshe et al., 2006; Lam et al., 2008; Boutte et al., 2010). However, the intracellular NtPPME1-GFP-positive organelles were clearly separate from endocytic endosomes, which were stained by FM4-64 after 10-min uptake in dividing BY2 cells (Fig. 4A1). When the cells were treated with BFA, FM4-64 stained endocytic vesicles formed large aggregates as previously reported (Robinson et al., 2008; Lam et al., 2009; Wang et al., 2010a), but NtPPME1-GFP labeled organelles in the cytosol remained punctate and showed no significant responses to BFA (Fig. 4A2). In contrast to NtPPME1-GFP-positive, FM4-64-stained endocytic vesicles fully colocalized with GFP-AtSCAMP4 in the cytosol after 10-min uptake and both formed BFA-induced aggregates (Fig. 4A, 3 and 4). To identify the sequential recruitments of endocytic and secretory materials during cell plate initiation, we next performed time-lapse imaging of cell plate initiation and traced the appearance of FM4-64 and NtPPME1-GFP signals at the cell plate. As shown in Figure 4B, a time course of images showed at the early stage of cell plate initiation and formation, FM4-64 stained endocytic vesicles reaching the cell plate prior to NtPPME1-GFP. This result may suggests that membrane materials via endocytosis are first recruited for cell plate membrane formation and afterward, the cell wall modifying enzyme NtPME1 is subsequently secreted into the existing cell plate for cell wall modification.

To further confirm the subcellular localization of NtPPME1 in dividing BY2 cells, we re-examined its subcellular distribution by confocal microscopy using different antibodies against organelle markers in fixed transgenic BY2 cells expressing NtPPME1-GFP. NtPPME1-GFP signals were detected on cell plates and some cytosolic punctate compartments, which fully colocalized with the NtPPME1 antibody labeling (Supplemental Fig. S5A). However, NtPPME1-GFP-positive cytosolic compartments were separate from the TGN marker OsSCAMP1, the Golgi apparatus marker AtEMP12, the clathrin-coated vesicle marker CHC, the PVC marker VSR, the methylesterified pectin marker JIM7, the de-methylesterified pectin marker JIM5, and the cytokinesis-specific syntaxin KNOLLE (Supplemental Fig. S5, B–H). Taken together, our results indicate that the NtPPME1-GFP-positive organelle mediates a polar protein secretion pathway from

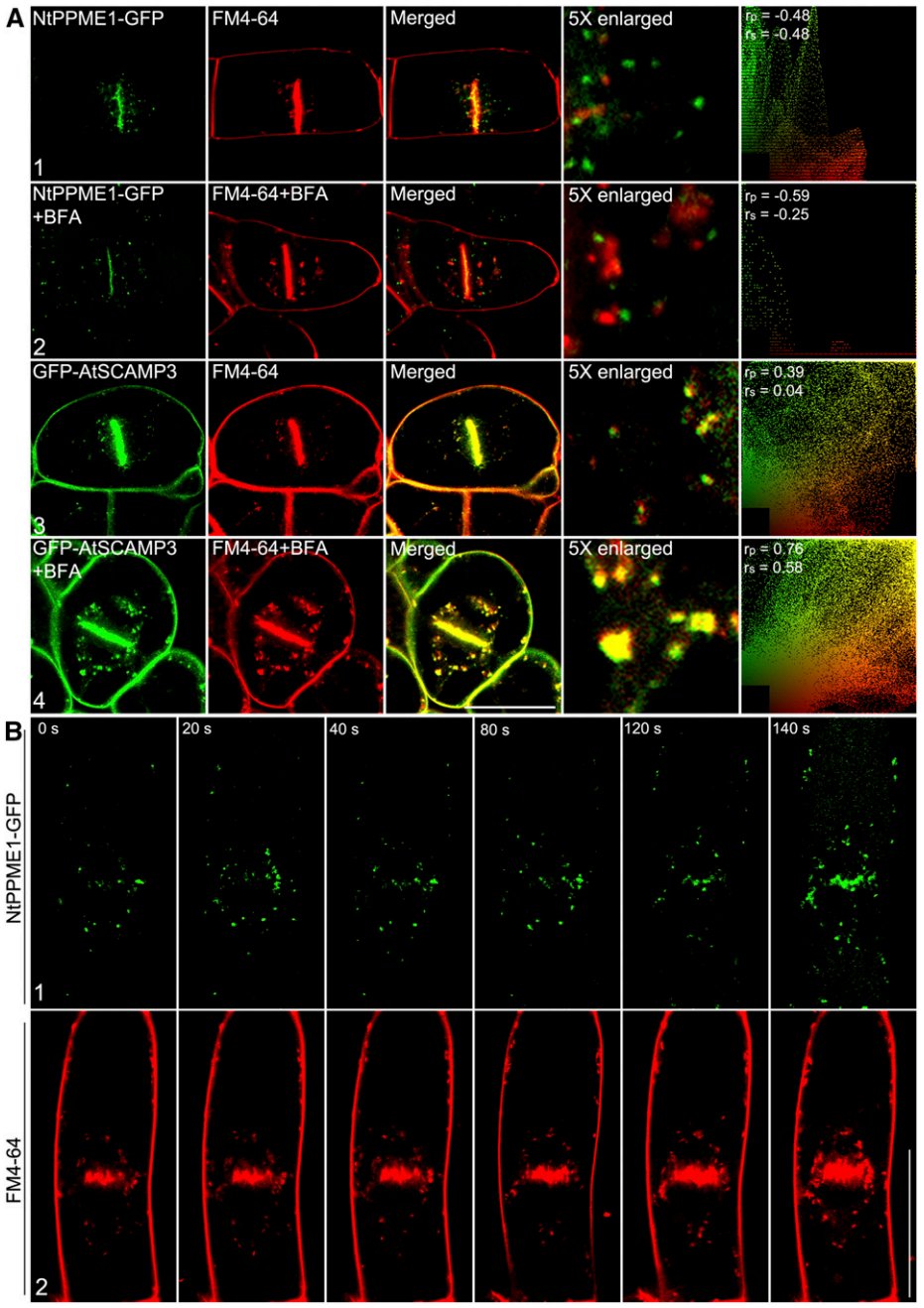

Figure 4. Polar secretion of NtPPME that contributes to cell plate formation during cytokinesis is distinct from the endocytic pathway in tobacco BY2 cells. A, Polar secretion of NtPPME1 was not overlapped with endocytic dye FM4-64 (1) and insensitive to the 10 μg mL^{-1} BFA treatment (2). Transgenic tobacco BY2 cells expressing GFP-AtSCAMP3 used as a control (3 and 4). Scale bar = 50 μm. B, Time-lapse images of cell plate initiation and formation in tobacco BY2 cell. (1) NtPPME1-GFP on the forming cell plate. (2) FM4-64-labeled endocytic membrane on the forming cell plate. Scale bar = 75 μm. The ImageJ program with the PSC colocalization plug-in (see "Materials and Methods") was used to calculate the colocalizations between these two fluorophores. Results are presented either as Pearson correlation coefficients or as Spearman's rank correlation coefficients, both of which produce r values in the range −1 to 1, where 0 indicates no discernable correlation while +1 and −1 indicate strong positive or negative correlations, respectively.

Golgi-to-CP, which is distinct from the classical Golgi-TGN-CP pathway.

Immunogold EM Identification of Golgi-Derived Secretion Vesicle as a Polarity-Associated Exocytic Vesicle for NtPPME1 Secretion to Pollen Tube Tip and the Cell Plate during Cytokinesis

To further morphologically characterize the NtPPME1-GFP labeled intracellular compartments during pollen tube growth and cell plate formation, we performed immunogold EM using the NtPPME1 antibody on ultrathin sections of high-pressure frozen/freeze-substituted samples of 2-h germinated pollen tubes and synchronized wild-type BY2 cells. An overview image of a pollen tube tip with a large number of accumulated exo-/endocytic vesicles is shown in Figure 5A1. The NtPPME1 antibodies labeled the vesicles in the pollen tube tip (Fig. 5A2). It is more challenging to preserve the pollen tube cell structures probably due to the relevant dense cell contents and vigorous cytoplasmic streaming. To better discern the fine structural details of the pollen tube, high-pressure fixed pollen tubes were subsequently treated with 2% osmium tetroxide during the freeze substitution procedures. A representative

structural image of the Golgi apparatus and TGN in a pollen tube is given in Figure 5A3. A typical image of a GDSV (~80 nm in diameter) was observed budding from the transside of the Golgi (indicated by an arrow) and separated from the TGN. Further immunogold labeling with NtPPME1 antibodies revealed GDSV (indicated by arrow), which was usually found budding from the transside of Golgi stacks (Fig. 5A4). An representative structural image of the TGN in pollen tube labeled with OsSCAMP1 antibodies is shown in Supplemental Figure S6A. Table I presents the quantitative results from static images and indicates that NtPPME1 is concentrated in the GDSVs budding from the *trans*side Golgi (38.7% of total account) compared with the gold particles labeled on TGNs (3.6% of total account). In contrast, OsSCAMP1 is concentrated on TGNs (42.8% of total account), but not on GDSVs (0.7% of total account) in the pollen tube (Table I).

In dividing BY2 cells, GDSVs budding from the transside of the Golgi were specifically labeled by NtPPME1 antibodies (arrows) as shown in Figure 5B1, but were absent from TGNs. Double immunogold EM with NtPPME1 and OsSCAMP1 antibodies showed GDSVs budding from the Golgi apparatus were labeled by NtPPME1 antibodies, whereas the TGN was specifically recognized by OsSCAMP1 antibodies (Fig. 5B3). A representative structural image of the TGN in a BY2 cell labeled with OsSCAMP1 antibodies is given in Supplemental Figure S6B. In addition, the forming cell plate in BY2 cells was also positively labeled with NtPPME1 antibodies (arrows), as shown in Figure 5B2. As expected, we found that NtPPME1-positive vesicles (indicated by arrows) were distinct from clathrin-coated vesicles (CCVs) labeled by CHC antibodies (indicated by arrowheads; Fig. 5B, 4–6). The distribution of immunogold labeling with antibodies against NtPPME1, OsSCAMP1, CHC, VSR, and AtEMP12 was quantitated based on the static images (Table II). The results obtained suggest that NtPPME1 resides on GDSV, which is a distinct exocytic compartment from Golgi apparatus, TGN, CCV, and multivesicular body (MVB). Thus, these results indicate that GDSV serve as a secretory organelle mediating the polar trafficking of NtPPME1 directly from the Golgi apparatus to PM/CP for cell wall formation during pollen tube tip expansion and cell plate formation.

ROP1 Activity Controls NtPPME1 Polar Exocytic Secretion and Targeting during Cell Plate Formation and Pollen Tube Growth

ROP GTPase signaling plays a key role in terms of its regulation of cell polarity, polar growth, and morphogenesis via the targeting of the cytoskeleton and vesicular trafficking in plant cells (Gu et al., 2005; Lee et al., 2008; Fu et al., 2009). To explore the mechanism that regulates GDSV-mediated NtPPME1 polar trafficking in pollen tube growth and cell plate formation, we tested the functions of ROP1 in regulating NtPPME1 localization and targeting. Transgenic BY2 cells expressing NtPPME1-GFP were synchronized and subsequently bombarded with RFP-CA-rop1 and RFP-DN-rop1, respectively (Supplemental Fig. S7). After incubation for 12 h, fluorescence recovery after photobleaching (FRAP) analysis studying the roles of ROP1 in exocytic targeting of NtPPME1-GFP to the cell plate was performed. A section of the whole cell plate was photobleached, and the recovery of NtPPME1-GFP fluorescence in the bleached region was monitored every 5 s. We reasoned that the recovery was caused by polar secretory activity to the cell plate. An example of the FRAP analysis of a BY2 cell expressing NtPPME1-GFP is shown in Figure 6A (top). Prior to photobleaching, NtPPME1-GFP appeared as a bright line in the middle of the BY2 cell (Fig. 6A, top). After photobleaching, the fluorescence signal in the cell plate area was reduced to ~3% of its original level (highlighted by the white cycle in Figure 6A, top). GFP signals started to reappear in the cell plate region within 45 s, reaching >85% of their original intensity 540 s after bleaching. The half-time of fluorescence recovery in the cell plate area was ~270 s ($n = 4$; Fig. 6C). The recovery of the GFP signal took place first at both edges of the cell plate and then gradually moved toward the center (Fig. 6A, top; Supplemental Movie S3). Furthermore, BY2 cells expressing NtPPME1-GFP coexpressed with CA-rop1 or DN-rop1 exhibited a different FRAP rate and pattern. CA-rop1 significantly increased the rate of fluorescence recovery. As shown in Figure 6A (middle), the GFP signals started to reappear in the cell plate region within 15 s, but the recovery of GFP signal intensity in the bleached cell plate region reached only ~40% of its original level 540 s after photobleaching ($n = 4$; Fig. 6C; Supplemental Movie S4). In contrast, DN-rop1 strongly

Table I. *Distribution of immunogold labeling with antibodies against NtPPME1 and OsSCAMP1 of tobacco pollen tubes*

To elucidate the distribution of the NtPPME1 antigens in GDSV, which is distinct from OsSCAMP1 antigen in the TGN, photographs of GDSV with distinguishable TGN, Golgi apparatus, endoplasmic reticulum (ER), and MVB were taken and the number of gold particles were counted for each individual organelle. Fifty-three GDSVs from different fixations of tobacco pollen tubes were evaluated for the label. Gp, Number of gold particles.

Antibody	GDSV	Tip Vesicle	TGN	Golgi	ER	MVB	Gp (%)
NtPPME1	175(38.7)	227 (50.3)	16 (3.6)	15 (3.1)	12 (2.6)	7 (1.7)	452 (100)
OsSCAMP1	5 (0.7)	298 (47)	217 (42.8)	20 (3.2)	17 (2.7)	22 (3.5)	579 (100)

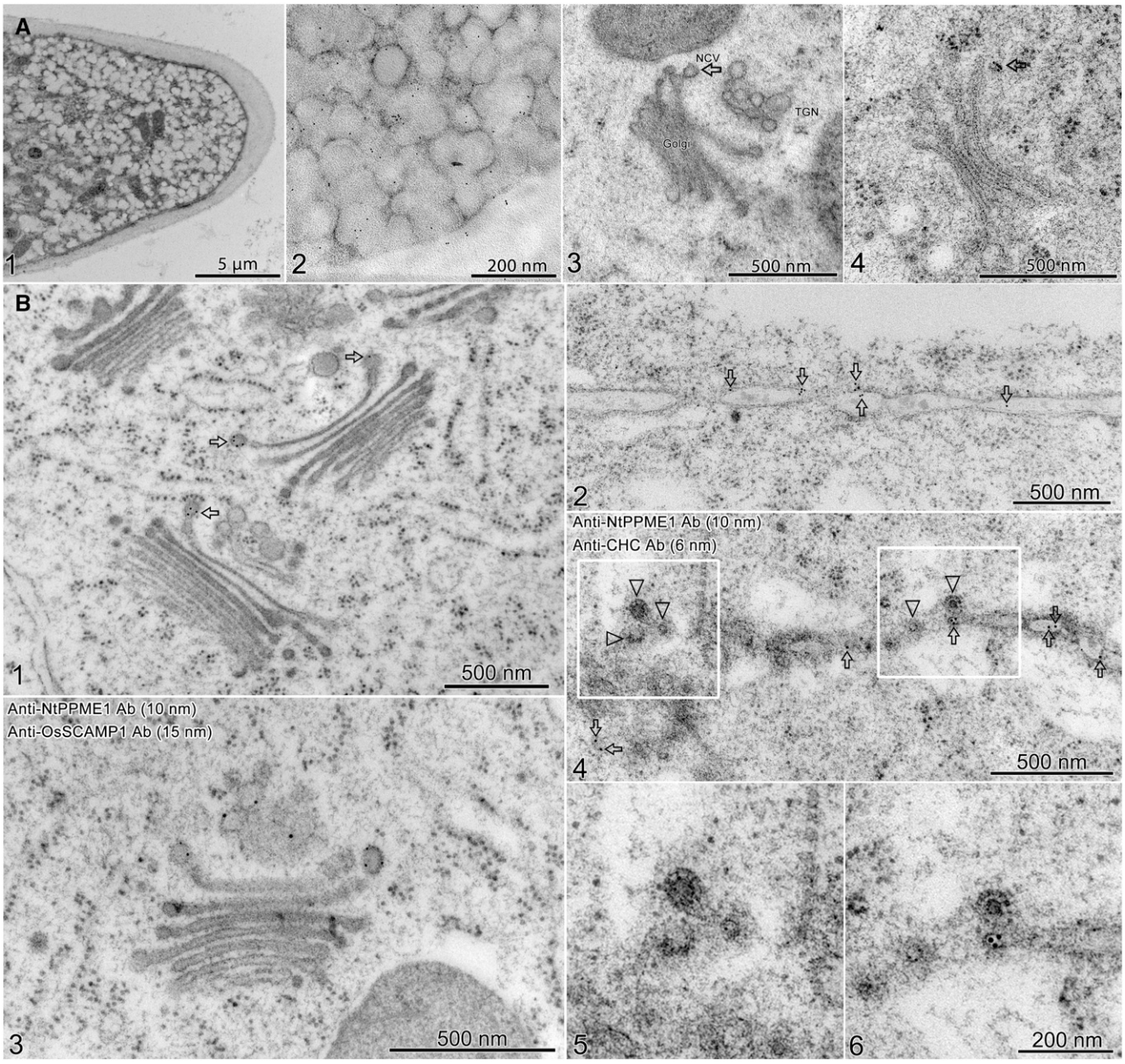

Figure 5. NtPPME1-defined GDSVs, independent from TGN and CCVs, contribute to pollen tube tip growth and cell plate formation in tobacco BY2 cells. High-pressure frozen/freeze-substituted samples of 2-h germinated pollen tubes and synchronized wild-type BY2 cells were used for immunolabeling. A, Pollen tubes were immunolabeled with NtPPME1 antibodies. (1) Overview of the ultrastructure of a tobacco pollen tube tip. (2) NtPPME1-labeled exocytic secretory vesicles accumulated in the pollen tube tip region. (3) Ultrastructure of secretory vesicle which is directly derived from Golgi apparatus and is distinct from the TGN. (4) NtPPME1 labeled the GDSVs near the Golgi apparatus. B, ImmunoEM of synchronized BY2 cells. (1) NtPPME1 antibodies specifically labeled GDSVs (arrows), but not TGN or TGN-derived CCVs. (2) NtPPME1 antibody labeled the cell plate in BY2 cells (arrows). (3) BY2 cells were double-labeled with NtPPME1 and TGN marker OsSCAMP1 antibodies. NtPPME1-labeled GDSVs (10 nm, indicated by arrows) were distinct from TGN, which was labeled by OsSCAMP1 antibody (15 nm, indicated by arrowheads). (4) NtPPME1 antibody labeled secretion vesicles on cell plate (10 nm, arrows) were separate from CHC antibody-labeled CCVs on or near the cell plate (6 nm, arrowheads). 5 and 6 are enlarged areas from 4.

inhibited the rate of fluorescence recovery (Fig. 6A, bottom). The GFP signals started to reappear in the cell plate region only after 1080 s. In addition, the recovery of GFP signal intensity in the bleached cell plate region reached only ~10% of its original level 540 s after photobleaching (n = 4; Fig. 6C; Supplemental Movie S5). To better illustrate the role of ROP1 in controlling the polar targeting of NtPPME1 to the cell plate, GFP

Table II. *Distribution of immunogold labeling with antibodies against NtPPME1, OsSCAMP1, CHC, VSR, and AtEMP12 in BY2 cells*

To elucidate the distribution of the NtPPME1 antigens in the GDSV, photographs of GDSV with distinguishable TGN, CCV, Golgi apparatus, and MVB were taken and the number of gold particles was counted for each individual organelle. Forty-four GDSVs from different fixations of BY2 cells were evaluated for the label. Gp, Number of gold particles; CHC, Clathrin H chain.

Antibody	GDSV	TGN	CCV	CP	Golgi	MVB	Gp (%)
NtPPME1	139 (38.2)	13 (3.6)	8 (2.2)	171 (47.0)	24 (6.6)	9 (2.5)	364 (100)
OsCAMP1	14 (3.6)	110 (27.9)	98 (24.9)	127 (32.2)	31 (7.9)	14 (3.6)	394 (100)
CHC	3 (1.7)	63 (35.2)	90 (50.3)	15 (25.7)	3 (1.68)	5 (2.79)	179 (100)
VSR	1 (1.5)	2 (3.0)	1 (1.5)	3 (4.5)	3 (4.5)	56 (84.8)	66 (100)
AtEMP12	2 (3.2)	6 (9.5)	1 (1.6)	4 (6.3)	44 (69.8)	6 (9.5)	63 (100)

signal intensities of the cell plate region after photobleaching were measured and displayed at 180 s from two directions, along the cell plate (indicated with a white line) and across the cell plate (indicated with a red line) as shown in Figure 6B. The cell plate started to recover, and the recovery pattern was from the two edges of the cell plate and then gradually moved to the central region (Fig. 6B1). CA-rop1 disrupted the GFP signal sequential recovery pattern, and the cell plate signal was partially recovered (Fig. 6B2). DN-rop1 strongly inhibited the GFP signal recovery on the cell plate (Fig. 6B3). To further demonstrate that the polar exocytosis and targeting of NtPPME1 to cell plate is ROP1-dependent, we treated BY2 cells expressing NtPPME1-GFP with 50 μM catechin-derivative (−)-epigallocatechin gallate (EGCG), a PME inhibitor (Lewis et al., 2008; Wolf et al., 2012), or coexpressed with CA-rop1 or DN-rop1, followed by confocal imaging. As shown in Supplemental Figure S8, the cell plate formation was strongly inhibited by treatment of the PME activity inhibitor EGCG, as well as by coexpression of DN-rop1 or CA-rop1.

Furthermore, ROP1 also controls the polar targeting of NtPPME1-GFP to the pollen tube tip and pollen tube growth (Fig. 6D). Expression of CA-rop1 disrupted the apical localization of NtPPME1-GFP, causing the pollen tube tip to swell and inhibiting pollen tube growth (Fig. 6D2). Expression of DN-rop1 abolished the apical localization of NtPPME1-GFP and inhibits pollen tube growth (Fig. 6D3). We also examined the effects of expression CA-rop1 and CA-rop1 at earlier stage of pollen tubes expressing NtPPME1-GFP. As shown in Supplemental Figure S9, expression of CA-rop1 or CA-rop1 abolished NtPPME1-GFP apical localization and strongly inhibited, but not completely stopped, pollen tube germination and growth (Supplemental Fig. S9). Taken together, these results suggest that ROP1 affects the polar targeting of NtPPME1 to the forming cell plate and growing pollen tube tip, which in turn regulates cell plate formation and pollen tube growth.

The exocytic targeting of SCAMP to PM has previously been shown to be achieved via the conventional Golgi-TGN-PM exocytosis pathway (Cai et al., 2011). Here we further tested the roles of ROP1 in controlling the polar targeting of SCAMP to PM in pollen tube (Supplemental Fig. S10). Our results suggest that ROP1 also participates in regulating the polar targeting of SCAMP by the conventional exocytosis pathway via TGN. Thus, it indicates that ROP1 may function as a master regulator for both conventional TGN-passing and GDSV-mediated exocytosis pathways in pollen tube growth and cell plate formation.

DISCUSSION

NtPPME1 Resides on a Polarity-Associated Exocytic Vesicle

In plants, pectin modifications by PMEs are usually accompanied with changes in plasticity, pH, and ionic contents of the cell wall, and finally influence plant cell growth and development (Micheli, 2001; Peaucelle et al., 2011). Previous studies indicate that NtPPME1 plays essential roles in pollen tube apical cell wall formation by determining its rigidity via demethylesterification of pectins (Bosch et al., 2005; Fayant et al., 2010; Chebli et al., 2012; Wang et al., 2013; Bidhendi and Geitmann, 2016). However, the subcellular localization and polar exocytosis of NtPPME1 remains unexplored. In addition, although pectins are also found to be abundant in the forming cell plate during cytokinesis, the involvement and functions of PMEs in the cell plate formation remain to be characterized (Baluska et al., 2005; Dhonukshe et al., 2006).

In this study, transgenic tobacco BY2 cells expressing NtPPME1-GFP were generated. The functional involvement and localization of NtPPME1 in cytokinesis was examined. The subcellular localization and dynamics of NtPPME1 in growing pollen tubes and cell plate formation (Figs. 1 and 3) suggest that the exocytosis and targeting of NtPPME1 for cell wall formation is closely associated with cell polarity in both cell expansion and cytokinesis. Further characterization of the NtPPME1 punctae in the cytoplasm of pollen tubes and dividing BY2 cells shows that NtPPME1 resides on a polar exocytic vesicle directly derived from transside Golgi (Fig. 5). GDSVs have previously been morphologically detected by 3D tomogram reconstruction and modeling (Kang et al., 2011; Gao et al., 2014b).

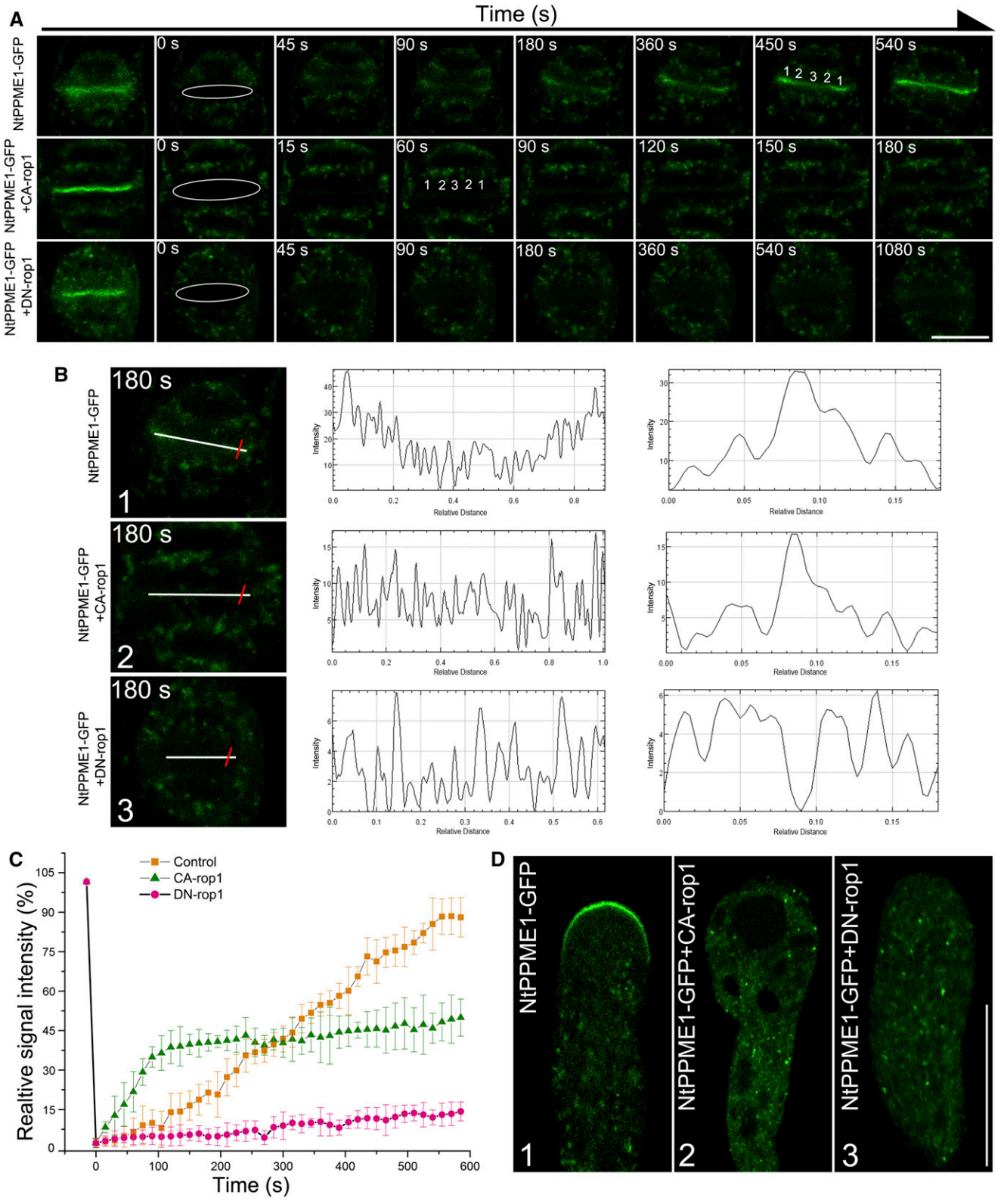

Figure 6. ROP1 regulates NtPPME1 polar exocytic secretion and targeting in cell wall formation during cytokinesis and pollen tube growth. A, FRAP analysis of NtPPME1-GFP highlighted cell plate formation (top) or coexpressed with CA-rop1 (middle) or DN-rop1 (bottom) during cytokinesis in tobacco BY2 cells. A series of images were shown before bleaching, immediately after bleaching (0 s), and then recovery of fluorescence was shown after bleaching at the indicated time points. Numbers indicate the

However, little is known about their biological functions in mediating protein trafficking. In our study, we have used NtPPME1 as a marker to reveal that GDSV mediates polar exocytosis of NtPPME1 for the cell wall formation. This is supported by several lines of evidence: (1) Both confocal microscopy and super-resolution imaging have shown that the NtPPME1-GFP-positive intracellular compartment is distinct from various endosomal markers involved in the conventional Golgi-TGN-PM exocytosis (Figs. 3 and 4; see Supplemental Figs. S2 and S5). (2) Pharmaceutical treatments with BFA, wortmannin, and ConcA have been well-established and are regularly used as a tool to influence conventional secretion, degradation, or endocytic organelles/vesicles in previous studies (Tse et al., 2004; Robinson et al., 2008; Lam et al., 2009; Cai et al., 2011; Scheuring et al., 2011; Gao et al., 2015; Cui et al., 2016). Drug treatments of the pollen tubes and BY2 cells expressing NtPPME1-GFP showed no obvious effects on NtPPME1-GFP labeled intracellular compartments except for disruption of the apical localization of NtPPME1 in pollen tube, which is likely to be caused by pollen tube growth arrest and cell polarity lost after the treatments (Fig. 2; Supplemental Fig. S3). In addition, the distinct responses and subcellular localizations between NtPPME1 and SCAMP after BFA and ConcA treatments also rule out the possibility that the intracellular NtPPME1-positive compartments might be derived from different functional domains of TGN or TGN-derived exocytic vesicles (Figs. 2, 3, and 4). (3) Ultrastructural analysis by immunogold EM with NtPPME1 antibodies have demonstrated that NtPPME1 resides on GDSVs that are distinct from the TGN in both pollen tube and tobacco BY2 cells (Fig. 5). Taken together, our results demonstrate that the polar exocytosis of NtPPME1 for cell wall rigidity modifications is mediated by a Golgi directly derived transport compartment, GDSV, in pollen tube growth and cell plate formation.

Polar Cellular Trafficking of NtPPME1 Highlights Golgi-PM Exocytosis Pathway Bypassing the TGN

It is generally considered that exocytic vesicles originate from the Golgi as most of the cell wall formation materials like pectins are first methlyesterified in the Golgi first and are then delivered to the pollen tube tip to meet the requirements of cell wall expansion (Carter et al., 2004; Lam et al., 2007b; Bove et al., 2008; Cai and Cresti, 2009; Hepler et al., 2013). However, whether these exocytic vesicles are solely derived from conventional Golgi-TGN-PM exocytic pathway or are possibly derived from other, unconventional, exocytic processes remains unknown.

Unconventional protein secretion (UPS) pathways are known and well-documented in yeast and mammalian cells, but recent studies suggest that UPS also exists in plant cells (Ding et al., 2012; Robinson et al., 2016). Although it is not known exactly how many different types of UPS pathways exist in plant cells, studies of exocyst-positive organelle (EXPO)-mediated UPS indicate that multiple exocytosis pathways may possibly co-operate and compensate for the classical endoplasmic reticulum-Golgi-TGN-PM protein exocytosis pathway (Wang et al., 2010b). Additionally, recent studies have shown the existence of different populations of exocyst-positive organelles mediating multiple post-Golgi transport routes from Golgi apparatus or TGN to PM/CW (Crowell et al., 2009; De Caroli et al., 2011; Boutte et al., 2013; McFarlane et al., 2013; Poulsen et al., 2014). Our results suggests that polar exocytosis of NtPPME1 along the Golgi-to-PM/CP pathway bypassing TGN, may complement the conventional Golgi-TGN-PM secretion pathway as with UPS. Our findings thus support that NtPPME1 is exocytotically secreted to the PM directly from trans-Golgi via GDSV. It will be technically challenging in future research to find out if the NtPPME1 secretion might involve other intermediate compartments or if NtPPME1 transiently and rapidly passes through TGN. Moreover, previous studies have shown that SCAMP is localized on the tubular-vesicular structures TGN/EE and its post-Golgi trafficking is clathrin-dependent (Lam et al., 2007a). SCAMP has been well-defined and used as a TGN maker in addition to its PM localization (Lam et al., 2007a; Lam et al., 2008; Lam et al., 2009; Wang et al., 2010a; Cai et al., 2011; Gao et al., 2012). Interestingly, Toyooka et al. (2009) described the secretory vesicle cluster (SVC), which is derived from TGN and consists of a cluster of vesicles often near TGN, as a distinct secretory compartment mediating targeting of

Figure 6. (*Continued.*)
order of signal recovery. Scale bar = 50 μm. B, Fluorescence-intensity recovery analysis of images in transgenic tobacco BY2 cell expressing NtPPME1-GFP (1), or coexpressed with CA-rop1 (2) or DN-rop1 (3) at 180 s after bleaching. The corresponding fluorescence intensity recovery along the cell plate (white line) was shown in the middle column and the fluorescence intensity recovery across the cell plate (red line) was indicated on the third column. C, Quantitative analysis of FRAP for A. Fluorescence recovery was measured by calculating the mean GFP signal intensity on the cell plate of the region of interest. For the top, fluorescence of the cell plate area recovered completely in 540 s, with a 270 $\pm$ 10 s half-time of recovery (■). For the middle, fluorescence at the cell plate area recovered dramatically without sequential order in 120 s, with a 60 $\pm$ 10 s half-time of recovery (▲). The fluorescent intensity of recovered cell plate is lower than that of the NtPPME1-GFP-highlighted cell plate alone. In contrast, little fluorescence recovery occurred in the cell plate area when coexpresssed with DN-rop1 (●). Similar results were obtained from four individual experiments. D, Confocal images showing the apical targeting of NtPPME1-GFP was inhibited when coexpressed with CA-rop1 (2) or DN-rop1 (3) in growing pollen tube. Scale bar = 25 μm.

SCAMP2 to PM. GDSVs are morphologically different from SVCs and are usually found near the trans-Golgi without clustering (Fig. 5). GDSVs mediate intracellular trafficking and targeting of NtPPME1 but are different from the secretory vesicles, which were labeled by JIM5 and JIM7 (Supplemental Fig. S5), whereas SVC contains cell wall components such as JIM7. These results also support the previous hypothesis that pectin and PME are packed and secreted by different intracellular vesicles so as to avoid earlier interactions between the enzyme and it substrate (Micheli, 2001). Recent studies show that cell plate formation also needs cell surface material, including cell wall components, which is rapidly delivered to the forming cell plate via endocytosis (Dhonukshe et al., 2006; Kim and Brandizzi, 2014). Therefore, JIM5 labeled intracellular compartments containing de-methylesterified pectins are likely endocytic in nature, seperate from the NtPPME1-GFP-positive exocytic compartments.

SCAMP also highlights the forming cell plate during cytokinesis and colocalized with the internalized endosomal marker FM4-64 on the forming cell plate during cell division (Lam et al., 2007a, 2007b; Lam et al., 2008). However, when compared with GFP-AtSCAMP3 and the endocytic endosomal marker FM4-64, NtPPME1-GFP punctae in pollen tubes and dividing BY2 cells are distinct from the classical TGNs/EEs, which usually bear clathrin coats (Figs. 2, 3, and 4). Furthermore, these NtPPME1-GFP-positive cytosolic punctae are insensitive to most pharmaceutical treatments, which affect either the secretion, recycling or endocytic pathways.

During cytokinesis, plant cells require specific proteins (e.g. KNOLLE and Rab GTPase) to guard the polar delivery, docking and fusion of vesicles carrying wall materials to the forming cell plate (Lukowitz et al., 1996). Meanwhile, organelles especially the Golgi apparatus relocate near the cell plate to aid secretion. Interestingly, we found that the signals of NtPPME1-GFP on the cell plate during cytokinesis are separated from cytokinesis-specific syntaxin KNOLLE, which is reported to be BFA sensitive (Boutte et al., 2010; Supplemental Fig. S5B8). This may indicate that cell plate formation may need specific types of secretion vesicles like GSDVs as the complemental exocytosis pathway.

ROP1 Regulates Polar Exocytosis of NtPPME1

In trying to understand the underlying mechanisms of the polarity-associated exocytosis of NtPPME1 in cell wall formation during cell expansion and cell cytokinesis, we tested and found that ROP1 may function as an essential regulator in controlling GDSV-mediated polar targeting of NtPPME1 to the pollen tube tip and cell plate (Fig. 6). The behavior and function of the highly dynamic populations of apical F-actin, which localizes to the tip region of the pollen tube, are regulated by ROP1 signaling network. CA-rop1 will enhance the accumulation of exocytic vesicles to the apical cortex of pollen tubes, leading to balloon-shaped tip and resulting in cell polarity lost. Expression of DN-rop1 can promote disassembly of F-actin and prevent polar exocytic vesicle transport and fusion with the apical PM (Lee et al., 2008; Fu et al., 2009). However, the origins and identities of these polar exocytic vesicles regulated by ROP1 remain elusive.

We previously demonstrated that the tip localization of NtPPME1 in the growing pollen tube is apical F-actin dependent. Disruption of apical F-actin organization and structures will abolish the tip localization of NtPPME1 and alter the cell wall rigidity (Wang et al., 2013). In this study, we found that ROP1 acts as an essential regulator in controlling the polar exocytosis of GDSV-mediated NtPPME1 and its targeting to the apical PM in growing pollen tubes. Expression of either CA-rop1 or DN-rop1 abolished the tip localization of NtPPME1-GFP and strongly inhibited pollen tube growth (Fig. 6D). NtPPME1-GFP is strictly focused on the pollen tube tip, and its expression intensity is closely associated with pollen tube polarity and growth oscillation (Wang et al., 2013). In addition to the GDSV-mediated NtPPME1 polar exocytosis pathway, the conventional Golgi-TGN-PM exocytic process, which mediates SCAMP secretion and targeting to PM, was also found to be controlled by ROP1 (Supplemental Fig. S10).

Besides the roles of ROP1 in controlling pollen tube growth, recent studies suggest ROPs might also participate in other cell polarization processes (Yang and Lavagi, 2012). Cell plate formation in plant cells is assisted by the insertion of plant-specific polarized proteins/membrane to the forming sites (Bednarek and Falbel, 2002; Jurgens, 2005; Backues et al., 2007). However, evidence for a function of ROPs in cell plate formation has not been reported, although overexpression of fluorescence-labeled ROP4 shows a localization at the forming cell plate (Molendijk et al., 2001).

By using FRAP analysis, we have shown that NtPPME1-mediated polar secretion and fusion with the cell plate is highly active at the growing edges of the cell plate and the NtPPME1-GFP signals recovered from the two edges sequentially to the central region of the forming cell plate. Interestingly, although CA-rop1 expression induced depolarization of cell plate signal recovery, it greatly accelerated the rate of recovery of NtPPME1 to the cell plate. In contrast, DN-rop1 expression significantly suppressed the polar secretion and targeting of NtPPME1 to the forming cell plate (Fig. 6, A–C). Therefore, our data provides a direct support for a crucial role of ROP1 in regulating polar exocytosis and targeting of GDSVs to the forming cell plate during cytokinesis. This further confirms a more general master role of ROP1 in the regulation of plant cell polarity.

In summary, we have identified an alternative Golgi-to-PM polar exocytosis via the GDSV, which mediates the polar secretion of NtPPME1 to the apoplast for cell wall rigidity modification during pollen tube expansion and cell plate formation. Several important questions

will need to be addressed in future studies. For example, what is the biological significance of GDSV-mediated exocytosis? What are the molecular characteristics of GDSVs? How is PPME1 specifically sequestered in GDSVs rather than being included in secretory vesicles? What are its up-/down-regulatory effectors? Using a combination of biochemical, proteomic, cellular, and genetic approaches to address these questions in future studies, we will be able to understand more about this GDSV-mediated secretion pathway as well as its significance to cell polar morphogenesis and plant development.

MATERIALS AND METHODS

Plant Materials and Pollen Tube Germination

Tobacco (*Nicotiana tabacum*) plants were grown in the greenhouse at 22°C under a light cycle of 12 h light and 12 h dark. Fresh pollen grains were harvested before use. For pollen tube germination, pollen grains were suspended in tobacco pollen-specific germination medium containing 10% Suc, 0.01% boric acid, 1 mM $CaCl_2$, 1 mM $Ca(NO_4)_2 \cdot H_2O$, 1 mM $MgSO_4 \cdot 7H_2O$ (pH 6.5) at 27.5°C for 2 h.

Particle Bombardment of Tobacco Pollens and BY2 Cells

For tobacco pollens, fresh anthers were harvested from 10 to 12 tobacco flowers and transferred into 20 mL of pollen germination medium. They were vortexed vigorously to release pollen grains into the germination medium. Pollen grain preparation and subsequent transient expression of proteins in the growing pollen tube via particle bombardment were carried out as previously described (Wang and Jiang, 2011a). For BY2 cells, in order to increase the expression efficiency in dividing BY2 cells, cell synchronization was first performed as previously described (Kumagai-Sano et al., 2006). The synchronized BY2 cells were then vacuum-filtered onto a filter paper and placed in the center of a Petri dish with BY2 culture agar medium. The sequential procedures for gene delivery into BY2 cells via particle bombardment were the same with the steps for pollen tube bombardment. The bombarded cells were kept in dark in plant growth chamber (27°C) for 8 to 12 h prior to observation for fluorescent signals.

Electron Microscopy of the Resin-Embedded Cells

The general procedures for TEM sample preparation and ultra-thin sectioning of samples were as previously described (Tse et al., 2004). For pollen tubes and BY2 cells, high-pressure freezing and substitution were carried out as previously described (Wang et al., 2013). Subsequent freeze substitution was carried out in dry acetone containing 0.1% uranyl acetate at −85°C. Infiltration with HM20, embedding, and UV polymerization were performed stepwise at −35°C. For immunolabeling, standard procedures were performed as described previously (Cui et al., 2014). The working concentration of affinity-purified antibodies is 40 μg/mL. Gold particle-coupled secondary antibodies were diluted 1:50, followed by the poststaining procedure by aqueous uranyl acetate/lead citrate. Ultrathin sections were examined using a Hitachi H-7650 transmission electron microscope with a CCD camera operating at 80 kV (Hitachi High-Technologies Corporation).

Immunofluorescence Labeling and Confocal Imaging

Fixation and preparation of BY2 cells/pollen tubes and subsequent labeling with antibodies and analysis by immunofluorescence were performed as previously described (Tse et al., 2004; Zhuang and Jiang, 2014). In general, the confocal fluorescence images were collected using a Leica TCS SP8 system with the following parameters: 63× water objective, 2× zoom, 900 gain, 0 background, 0.168 μm pixel size, and photomultiplier tubes detector. The images from pollen tubes labeled with antibodies were collected with a laser level of ≤ 3% to ensure that the fluorescent signal was within the linear range of detection (typically 0.5% or 1% laser was used). Colocalizations between two fluorophores were calculated by using ImageJ program with the PSC colocalization plug-in (French et al., 2008). Results are presented either as Pearson correlation coefficients or as Spearman's rank correlation coefficients, both of which produce r values in the range (−1 to 1), where 0 indicates no discernable correlation while +1 and −1 indicate strong positive and negative correlations, respectively.

Superresolution Microscopy Imaging by STORM

The two-channel STORM was built upon a Nikon Ti-E inverted microscope basing with perfect focus system. Laser excitations for Alexa 647 channel and Alexa 750 channel were provided by a 656.5 nm DPSS laser and a 750 nm diode laser, respectively. The fluorescent signals of both channels were collected by a 100× TIRF objective (Nikon) and passed through a home-built channel splitter before simultaneously forming images on an EMCCD (Andor, IXon-Ultra). One emission filter was placed in each path of the channel to block the excitation laser. To stabilize the sample, the perfect focus system was used to lock the focus, and the sample drift was measured with the brightfield image of cells via a third channel and then was compensated in real time by an x-y piezo stage (PIP545.R7.XYZ). All measurement, control, and acquisition were done using custom written software. Prior to STORM imaging, the desired position is located using conventional fluorescence image with relatively low laser excitation power, typically 60W/cm^2 for a 656.5 nm laser in an Alexa 647 channel and 80W/cm^2 for a 750 nm laser in an Alexa 750 nm channel. During the STORM acquisition, the laser power was raised to 2kW/cm^2 and 4.5kW/cm^2, respectively. Blinking signals of both channels were recorded simultaneously using EMCCD with 100× EM gain at 30 frames per second for 30,000 frames. The data were then analyzed by using Gaussian fitting software to reconstruct the superresolution image. Throughout STORM experiments, the highly inclined and laminated optical sheet geometry (Tokunaga et al., 2008; Wang, 2016) was applied so that the illuminated area in cell is confined to a 3 μm thick sheet 10 μm above the coverslip, thus effectively reducing the background caused by out-of-focus signal. All cells for STORM imaging were immobilized on poly-Lys coated coverslip and mounted in STORM imaging buffer: 200 mM Tris-Cl (pH 9.0; Sigma-Aldrich, T2819) containing 10% (w/v) Glc (Sigma-Aldrich, G8270), 0.56 mg/mL Glc oxidase (Sigma-Aldrich, G2133), 57 μg/mL catalase (Sigma-Aldrich, C3515), 2 mM cyclooctatetraene (TCI, C0505, dissolved in DMSO), 25 mM TCEP (Sigma, 646547), 1 mM ascorbic acid (TCI, A0537), and 1 mM Methyl Viologen (Sigma-Aldrich, 856177).

Drug Treatment and Antibodies

Stock solutions of wortmannin (1 mM in DMSO; Sigma-Aldrich), BFA (1 mM in DMSO; Sigma-Aldrich), FM4-64 (4 mM in DMSO; Invitrogen), ConcA (1 mM in DMSO; Sigma-Aldrich), and catechin-derivative (−)-EGCG (5 mM in H_2O, Sigma-Aldrich) were prepared. These drugs were diluted in germination medium to appropriate working concentrations before incubation with germinating pollen tubes. For each drug treatment, germinating pollen tubes or BY2 cells were mixed with the drugs in working solutions in the medium at a 1:1 ratio to minimize sample variation, and such a method of drug treatment has been well-documented with success in both pollen tubes and BY2 cells of previous studies (Tse et al., 2004; Tse et al., 2006; Robinson et al., 2008; Lam et al., 2009; Wang et al., 2010a; Cai et al., 2011; Wang et al., 2011b; Zhuang et al., 2013; Cui et al., 2014; Ding et al., 2014; Gao et al., 2014b; Gao et al., 2015; Shen et al., 2016; Wang et al., 2016; Chung et al., 2016). The JIM5 and JIM7 antibodies were purchased from the Paul Knox Cell Wall Lab at the University of Leeds (Plant 710Probes).

A synthetic peptide (CQPTPYKQTCEKTLSSAKNASEPKDF) within the N terminus of tobacco NtPPME1 was synthesized (GenScript) and used as antigen to raise the antibody. The synthetic peptide was conjugated with keyhole limpet hemocyanin and used to immunize nine rats at the animal house of the Chinese University of Hong Kong (CUHK). The generated antibodies (anti-NtPPME1) were further affinity-purified with a CnBr-activated Sepharose (Sigma-Aldrich; catalog No. C9142-15G) column conjugated with synthetic peptides as described previously (Jiang and Rogers, 1998). AtVSR1, OsSCAMP1, and AtEMP12 antibodies were generated as previously described (Tse et al., 2004; Lam et al., 2007a; Gao et al., 2012). The JIM5, JIM7, and LM7 antibodies were purchased from the Paul Knox Cell Wall Lab at the University of Leeds (PlantProbes). A monoclonal antibody against CHC (at 250 mg/mL) was purchased from BD Bioscience (catalog no. C610500). A polyclonal antibody against KNOLLE was purchased from Agrisera AB (catalog no. AS06168).

Accession Numbers

Sequence data from this article can be found in the GenBank/EMBL data libraries under accession numbers NtPPME1(AY772945), AtVSR2 (NM_128582), AtSCAMP3 (At2g20840), and AtSCAMP4 (At1g03550).

Supplemental Data

The following supplemental materials are available.

Supplemental Figure S1. Characterization of the NtPPME1 antibody.

Supplemental Figure S2. NtPPME1-GFP-positive compartments are distinct from PVC, endocytic vesicle, TGN, and Golgi makers in growing pollen tubes.

Supplemental Figure S3. Quantification analysis of cell responses to the drug treatments.

Supplemental Figure S4. *NtPPME1* expression analysis in pollens and BY2 cells.

Supplemental Figure S5. NtPPME1-positive compartments are distinct from different organelle markers in tobacco BY2 Cells.

Supplemental Figure S6. Immunogold electron microscopy localization of SCAMP1 in pollen tubes and BY2 cells.

Supplemental Figure S7. Coexpression of NtPPME1-GFP with RFP-CA-rop1 or RFP-DN-rop1 in tobacco BY2 cells during cytokinesis.

Supplemental Figure S8. The effects of inhibition of PME activity and expression of CA-rop1 or DN-rop1 on NtPPME1-GFP polar exocytic targeting to the forming cell plate.

Supplemental Figure S9. Coexpression of NtPPME1-GFP with CA-rop1 or DN-rop1 in the early stages of pollen tube germination.

Supplemental Figure S10. FRAP of GFP-AtSCAMP4-stained apical PM in tobacco pollen tubes.

Supplemental Movie S1. Dynamics of NtPPME1-GFP in a growing pollen tube.

Supplemental Movie S2. NtPPME1-GFP highlights the forming cell plate in a dividing transgenic BY2 cell.

Supplemental Movie S3. FRAP analysis of NtPPME1-GFP at cell plate formation in BY2 cells.

Supplemental Movie S4. FRAP analysis of NtPPME1-GFP at cell plate formation in BY2 cells coexpressed with CA-rop1.

Supplemental Movie S5. FRAP analysis of NtPPME1-GFP at cell plate formation in BY2 cells coexpressed with DN-rop1.

ACKNOWLEDGMENTS

We thank Zhenbiao Yang (University of Califonia, Riverside) for sharing the rop1, DN-rop1, and CA-rop1 plasmids. Shengwang Du acknowledges the support from NanoBioImaging Ltd. through a research contract with HKUST R and D Corporation Ltd. (RDC14152140).

Received May 11, 2016; accepted August 8, 2016; published August 16, 2016.

LITERATURE CITED

Altartouri B, Geitmann A (2015) Understanding plant cell morphogenesis requires real-time monitoring of cell wall polymers. Curr Opin Plant Biol **23:** 76–82

Backues SK, Konopka CA, McMichael CM, Bednarek SY (2007) Bridging the divide between cytokinesis and cell expansion. Curr Opin Plant Biol **10:** 607–615

Baluska F, Menzel D, Barlow PW (2006) Cytokinesis in plant and animal cells: endosomes 'shut the door'. Dev Biol **294:** 1–10

Baluska F, Liners F, Hlavacka A, Schlicht M, Van Cutsem P, McCurdy DW, Menzel D (2005) Cell wall pectins and xyloglucans are internalized into dividing root cells and accumulate within cell plates during cytokinesis. Protoplasma **225:** 141–155

Bednarek SY, Falbel TG (2002) Membrane trafficking during plant cytokinesis. Traffic **3:** 621–629

Bidhendi AJ, Geitmann A (2016) Relating the mechanics of the primary plant cell wall to morphogenesis. J Exp Bot **67:** 449–461

Bosch M, Hepler PK (2006) Silencing of the tobacco pollen pectin methylesterase NtPPME1 results in retarded in vivo pollen tube growth. Planta **223:** 736–745

Bosch M, Cheung AY, Hepler PK (2005) Pectin methylesterase, a regulator of pollen tube growth. Plant Physiol **138:** 1334–1346

Boutté Y, Jonsson K, McFarlane HE, Johnson E, Gendre D, Swarup R, Friml J, Samuels L, Robert S, Bhalerao RP (2013) ECHIDNA-mediated post-Golgi trafficking of auxin carriers for differential cell elongation. Proc Natl Acad Sci USA **110:** 16259–16264

Boutté Y, Frescatada-Rosa M, Men S, Chow CM, Ebine K, Gustavsson A, Johansson L, Ueda T, Moore I, Jürgens G, Grebe M (2010) Endocytosis restricts Arabidopsis KNOLLE syntaxin to the cell division plane during late cytokinesis. EMBO J **29:** 546–558

Bove J, Vaillancourt B, Kroeger J, Hepler PK, Wiseman PW, Geitmann A (2008) Magnitude and direction of vesicle dynamics in growing pollen tubes using spatiotemporal image correlation spectroscopy and fluorescence recovery after photobleaching. Plant Physiol **147:** 1646–1658

Burkel BM, Benink HA, Vaughan EM, von Dassow G, Bement WM (2012) A Rho GTPase signal treadmill backs a contractile array. Dev Cell **23:** 384–396

Cai G, Cresti M (2009) Organelle motility in the pollen tube: a tale of 20 years. J Exp Bot **60:** 495–508

Cai Y, Jia T, Lam SK, Ding Y, Gao C, San MWY, Pimpl P, Jiang L (2011) Multiple cytosolic and transmembrane determinants are required for the trafficking of SCAMP1 via an ER-Golgi-TGN-PM pathway. Plant J **65:** 882–896

Carter CJ, Bednarek SY, Raikhel NV (2004) Membrane trafficking in plants: new discoveries and approaches. Curr Opin Plant Biol **7:** 701–707

Chebli Y, Kaneda M, Zerzour R, Geitmann A (2012) The cell wall of the Arabidopsis pollen tube–spatial distribution, recycling, and network formation of polysaccharides. Plant Physiol **160:** 1940–1955

Chung KP, Zeng Y, Jiang L (2016) COPII paralogs in plants: functional redundancy or diversity? Trends Plant Sci **21:** 758–769

Crowell EF, Bischoff V, Desprez T, Rolland A, Stierhof YD, Schumacher K, Gonneau M, Höfte H, Vernhettes S (2009) Pausing of Golgi bodies on microtubules regulates secretion of cellulose synthase complexes in Arabidopsis. Plant Cell **21:** 1141–1154

Cui Y, Shen J, Gao C, Zhuang X, Wang J, Jiang L (2016) Biogenesis of plant prevacuolar multivesicular bodies. Mol Plant **9:** 774–786

Cui Y, Zhao Q, Gao C, Ding Y, Zeng Y, Ueda T, Nakano A, Jiang L (2014) Activation of the Rab7 GTPase by the MON1-CCZ1 complex is essential for PVC-to-vacuole trafficking and plant growth in Arabidopsis. Plant Cell **26:** 2080–2097

De Caroli M, Lenucci MS, Di Sansebastiano GP, Dalessandro G, De Lorenzo G, Piro G (2011) Protein trafficking to the cell wall occurs through mechanisms distinguishable from default sorting in tobacco. Plant J **65:** 295–308

Dettmer J, Friml J (2011) Cell polarity in plants: when two do the same, it is not the same.... Curr Opin Cell Biol **23:** 686–696

Dhonukshe P, Baluska F, Schlicht M, Hlavacka A, Samaj J, Friml J, Gadella TW, Jr. (2006) Endocytosis of cell surface material mediates cell plate formation during plant cytokinesis. Dev Cell **10:** 137–150

Ding Y, Wang J, Wang J, Stierhof YD, Robinson DG, Jiang L (2012) Unconventional protein secretion. Trends Plant Sci **17:** 606–615

Ding Y, Wang J, Chun Lai JH, Ling Chan VH, Wang X, Cai Y, Tan X, Bao Y, Xia J, Robinson DG, Jiang L (2014) Exo70E2 is essential for exocyst subunit recruitment and EXPO formation in both plants and animals. Mol Biol Cell **25:** 412–426

Emans N, Zimmermann S, Fischer R (2002) Uptake of a fluorescent marker in plant cells is sensitive to brefeldin A and wortmannin. Plant Cell **14:** 71–86

Ethier MF, Madison JM (2002) LY294002, but not wortmannin, increases intracellular calcium and inhibits calcium transients in bovine and human airway smooth muscle cells. Cell Calcium **32:** 31–38

Fayant P, Girlanda O, Chebli Y, Aubin CE, Villemure I, Geitmann A (2010) Finite element model of polar growth in pollen tubes. Plant Cell **22:** 2579–2593

French AP, Mills S, Swarup R, Bennett MJ, Pridmore TP (2008) Colocalization of fluorescent markers in confocal microscope images of plant cells. Nat Protoc **3:** 619–628

Fu Y, Xu T, Zhu L, Wen M, Yang Z (2009) A ROP GTPase signaling pathway controls cortical microtubule ordering and cell expansion in Arabidopsis. Curr Biol **19:** 1827–1832

Gao C, Yu CKY, Qu S, San MWY, Li KY, Lo SW, Jiang L (2012) The Golgi-localized Arabidopsis endomembrane protein12 contains both endoplasmic reticulum export and Golgi retention signals at its C terminus. Plant Cell **24:** 2086–2104

Gao C, Cai Y, Wang Y, Kang BH, Aniento F, Robinson DG, Jiang L (2014b) Retention mechanisms for ER and Golgi membrane proteins. Trends Plant Sci **19:** 508–515

Gao C, Luo M, Zhao Q, Yang R, Cui Y, Zeng Y, Xia J, Jiang L (2014a) A unique plant ESCRT component, FREE1, regulates multivesicular body protein sorting and plant growth. Curr Biol **24:** 2556–2563

Gao C, Zhuang X, Cui Y, Fu X, He Y, Zhao Q, Zeng Y, Shen J, Luo M, Jiang L (2015) Dual roles of an Arabidopsis ESCRT component FREE1 in regulating vacuolar protein transport and autophagic degradation. Proc Natl Acad Sci USA **112:** 1886–1891

Gu Y, Fu Y, Dowd P, Li S, Vernoud V, Gilroy S, Yang Z (2005) A Rho family GTPase controls actin dynamics and tip growth via two counteracting downstream pathways in pollen tubes. J Cell Biol **169:** 127–138

Hepler PK, Rounds CM, Winship LJ (2013) Control of cell wall extensibility during pollen tube growth. Mol Plant **6:** 998–1017

Jaillais Y, Gaude T (2008) Plant cell polarity: sterols enter into action after cytokinesis. Dev Cell **14:** 318–320

Jiang L, Rogers JC (1998) Integral membrane protein sorting to vacuoles in plant cells: evidence for two pathways. J Cell Biol **143:** 1183–1199

Jiang L, Yang SL, Xie LF, Puah CS, Zhang XQ, Yang WC, Sundaresan V, Ye D (2005) VANGUARD1 encodes a pectin methylesterase that enhances pollen tube growth in the Arabidopsis style and transmitting tract. Plant Cell **17:** 584–596

Jürgens G (2005) Plant cytokinesis: fission by fusion. Trends Cell Biol **15:** 277–283

Kang BH, Nielsen E, Preuss ML, Mastronarde D, Staehelin LA (2011) Electron tomography of RabA4b- and PI-4Kβ1-labeled trans Golgi network compartments in Arabidopsis. Traffic **12:** 313–329

Kim SJ, Brandizzi F (2014) The plant secretory pathway: an essential factory for building the plant cell wall. Plant Cell Physiol **55:** 687–693

Kroeger J, Geitmann A (2012) The pollen tube paradigm revisited. Curr Opin Plant Biol **15:** 618–624

Kumagai-Sano F, Hayashi T, Sano T, Hasezawa S (2006) Cell cycle synchronization of tobacco BY-2 cells. Nat Protoc **1:** 2621–2627

Lam SK, Tse YC, Robinson DG, Jiang L (2007b) Tracking down the elusive early endosome. Trends Plant Sci **12:** 497–505

Lam SK, Cai Y, Hillmer S, Robinson DG, Jiang L (2008) SCAMPs highlight the developing cell plate during cytokinesis in tobacco BY-2 cells. Plant Physiol **147:** 1637–1645

Lam SK, Siu CL, Hillmer S, Jang S, An G, Robinson DG, Jiang L (2007a) Rice SCAMP1 defines clathrin-coated, trans-golgi-located tubular-vesicular structures as an early endosome in tobacco BY-2 cells. Plant Cell **19:** 296–319

Lam SK, Cai Y, Tse YC, Wang J, Law AH, Pimpl P, Chan HY, Xia J, Jiang L (2009) BFA-induced compartments from the Golgi apparatus and trans-Golgi network/early endosome are distinct in plant cells. Plant J **60:** 865–881

Lee YJ, Szumlanski A, Nielsen E, Yang Z (2008) Rho-GTPase-dependent filamentous actin dynamics coordinate vesicle targeting and exocytosis during tip growth. J Cell Biol **181:** 1155–1168

Lewis KC, Selzer T, Shahar C, Udi Y, Tworowski D, Sagi I (2008) Inhibition of pectin methyl esterase activity by green tea catechins. Phytochemistry **69:** 2586–2592

Li H, Friml J, Grunewald W (2012) Cell polarity: stretching prevents developmental cramps. Curr Biol **22:** R635–R637

Libault M, Brechenmacher L, Cheng J, Xu D, Stacey G (2010) Root hair systems biology. Trends Plant Sci **15:** 641–650

Lukowitz W, Mayer U, Jürgens G (1996) Cytokinesis in the Arabidopsis embryo involves the syntaxin-related KNOLLE gene product. Cell **84:** 61–71

McFarlane HE, Watanabe Y, Gendre D, Carruthers K, Levesque-Tremblay G, Haughn GW, Bhalerao RP, Samuels L (2013) Cell wall polysaccharides are mislocalized to the Vacuole in echidna mutants. Plant Cell Physiol **54:** 1867–1880

Micheli F (2001) Pectin methylesterases: cell wall enzymes with important roles in plant physiology. Trends Plant Sci **6:** 414–419

Molendijk AJ, Bischoff F, Rajendrakumar CS, Friml J, Braun M, Gilroy S, Palme K (2001) Arabidopsis thaliana Rop GTPases are localized to tips of root hairs and control polar growth. EMBO J **20:** 2779–2788

Moore PJ, Staehelin LA (1988) Immunogold localization of the cell-wall-matrix polysaccharides rhamnogalacturonan I and xyloglucan during cell expansion and cytokinesis inTrifolium pratense L.; implication for secretory pathways. Planta **174:** 433–445

Mravec J, Petrášek J, Li N, Boeren S, Karlova R, Kitakura S, Pařezová M, Naramoto S, Nodzyński T, Dhonukshe P, Bednarek SY, Zažímalová E, et al (2011) Cell plate restricted association of DRP1A and PIN proteins is required for cell polarity establishment in Arabidopsis. Curr Biol **21:** 1055–1060

Peaucelle A, Braybrook SA, Le Guillou L, Bron E, Kuhlemeier C, Höfte H (2011) Pectin-induced changes in cell wall mechanics underlie organ initiation in Arabidopsis. Curr Biol **21:** 1720–1726

Poulsen CP, Dilokpimol A, Mouille G, Burow M, Geshi N (2014) Arabinogalactan glycosyltransferases target to a unique subcellular compartment that may function in unconventional secretion in plants. Traffic **15:** 1219–1234

Ridley A (2013) GTPase switch: Ras then Rho and Rac. Nat Cell Biol **15:** 337

Robinson DG, Ding Y, Jiang L (2016) Unconventional protein secretion in plants: a critical assessment. Protoplasma **253:** 31–43

Robinson DG, Albrecht S, Moriysu Y (2004) The V-ATPase inhibitors concanamycin A and bafilomycin A lead to Golgi swelling in tobacco BY-2 cells. Protoplasma **224:** 255–260

Robinson DG, Langhans M, Saint-Jore-Dupas C, Hawes C (2008) BFA effects are tissue and not just plant specific. Trends Plant Sci **13:** 405–408

Röckel N, Wolf S, Kost B, Rausch T, Greiner S (2008) Elaborate spatial patterning of cell-wall PME and PMEI at the pollen tube tip involves PMEI endocytosis, and reflects the distribution of esterified and de-esterified pectins. Plant J **53:** 133–143

Scheuring D, Viotti C, Krüger F, Künzl F, Sturm S, Bubeck J, Hillmer S, Frigerio L, Robinson DG, Pimpl P, Schumacher K (2011) Multivesicular bodies mature from the trans-Golgi network/early endosome in Arabidopsis. Plant Cell **23:** 3463–3481

Shen J, Gao C, Zhao Q, Lin Y, Wang X, Zhuang X, Jiang L (2016) AtBRO1 functions in ESCRT-I complex to regulate multivescular bpdy protein sorting. Mol Plant **9:** 760–763

Tokunaga M, Imamoto N, Sakata-Sogawa K (2008) Highly inclined thin illumination enables clear single-molecule imaging in cells. Nat Methods **5:** 159–161

Toyooka K, Goto Y, Asatsuma S, Koizumi M, Mitsui T, Matsuoka K (2009) A mobile secretory vesicle cluster involved in mass transport from the Golgi to the plant cell exterior. Plant Cell **21:** 1212–1229

Tse YC, Lo SW, Hillmer S, Dupree P, Jiang L (2006) Dynamic response of prevacuolar compartments to brefeldin a in plant cells. Plant Physiol **142:** 1442–1459

Tse YC, Mo B, Hillmer S, Zhao M, Lo SW, Robinson DG, Jiang L (2004) Identification of multivesicular bodies as prevacuolar compartments in Nicotiana tabacum BY-2 cells. Plant Cell **16:** 672–693

Viotti C, Bubeck J, Stierhof YD, Krebs M, Langhans M, van den Berg W, van Dongen W, Richter S, Geldner N, Takano J, Jürgens G, de Vries SC, et al (2010) Endocytic and secretory traffic in Arabidopsis merge in the trans-Golgi network/early endosome, an independent and highly dynamic organelle. Plant Cell **22:** 1344–1357

Wang H (2016) Visualizing plant cells in a brand new way. Mol Plant **9:** 633–635

Wang H, Jiang L (2011a) Transient expression and analysis of fluorescent reporter proteins in plant pollen tubes. Nat Protoc **6:** 419–426

Wang H, Zhuang XH, Hillmer S, Robinson DG, Jiang LW (2011b) Vacuolar sorting receptor (VSR) proteins reach the plasma membrane in germinating pollen tubes. Mol Plant **4:** 845–853

Wang H, Zhuang X, Cai Y, Cheung AY, Jiang L (2013) Apical F-actin-regulated exocytic targeting of NtPPME1 is essential for construction and rigidity of the pollen tube cell wall. Plant J **76:** 367–379

Wang H, Tse YC, Law AH, Sun SS, Sun YB, Xu ZF, Hillmer S, Robinson DG, Jiang L (2010a) Vacuolar sorting receptors (VSRs) and secretory carrier membrane proteins (SCAMPs) are essential for pollen tube growth. Plant J **61:** 826–838

Wang J, Cai Y, Miao Y, Lam SK, Jiang L (2009) Wortmannin induces homotypic fusion of plant prevacuolar compartments. J Exp Bot **60:** 3075–3083

Wang J, Ding Y, Wang J, Hillmer S, Miao Y, Lo SW, Wang X, Robinson DG, Jiang L (2010b) EXPO, an exocyst-positive organelle distinct from multivesicular endosomes and autophagosomes, mediates cytosol to cell wall exocytosis in Arabidopsis and tobacco cells. Plant Cell **22:** 4009–4030

Wang J, Ding Y, Zhuang X, Hu S, Jiang L (2016) Protein co-localization studies: issues and considerations. Mol Plant **9:** 1221–1223

Wolf S, Mravec J, Greiner S, Mouille G, Höfte H (2012) Plant cell wall homeostasis is mediated by brassinosteroid feedback signaling. Curr Biol **22:** 1732–1737

Xu T, Wen M, Nagawa S, Fu Y, Chen JG, Wu MJ, Perrot-Rechenmann C, Friml J, Jones AM, Yang Z (2010) Cell surface- and rho GTPase-based auxin signaling controls cellular interdigitation in Arabidopsis. Cell **143:** 99–110

Yang Z, Lavagi I (2012) Spatial control of plasma membrane domains: ROP GTPase-based symmetry breaking. Curr Opin Plant Biol **15:** 601–607

Zhao Q, Gao C, Lee P, Liu L, Li S, Hu T, Shen J, Pan S, Ye H, Chen Y, Cao W, Cui Y, et al (2015) Fast-suppressor screening for new components in protein trafficking, organelle biogenesis and silencing pathway in Arabidopsis thaliana using DEX-inducible FREE1-RNAi plants. J Genet Genomics **42:** 319–330

Zhuang X, Jiang L (2014) Autophagosome biogenesis in plants: roles of SH3P2. Autophagy **10:** 704–705

Zhuang X, Wang H, Lam SK, Gao C, Wang X, Cai Y, Jiang L (2013) A BAR-domain protein SH3P2, which binds to phosphatidylinositol 3-phosphate and ATG8, regulates autophagosome formation in Arabidopsis. Plant Cell **25:** 4596–4615

Zonia L, Munnik T (2011) Understanding pollen tube growth: the hydrodynamic model versus the cell wall model. Trends Plant Sci **16:** 347–352